

PressLight: Learning Max Pressure Control for Signalized Intersections in Arterial Network

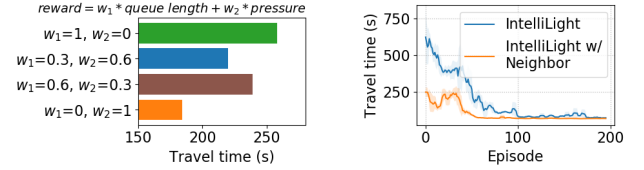
Hua Wei[†], Chacha Chen[‡], Guanjie Zheng[†], Kan Wu[†], Kai Xu[§], Vikash Gayah[†], Zhenhui Li[†]

[†]Pennsylvania State University, [‡]Shanghai Jiao Tong University, [§]Shanghai Tianrang Intelligent Technology Co., Ltd
[†]{hzw77, gjz5038, jessielj}@ist.psu.edu, [†]kxw5389@psu.edu, [†]gayah@engr.psu.edu, [‡]chacha1997@sjtu.edu.cn,
[§]kai.xu@tianrang-inc.com

ABSTRACT

Traffic signal control is essential for transportation efficiency in the road network. It has been a challenging problem because of the complexity in traffic dynamics. Conventional transportation research suffers from the incompetency to adapt to dynamic traffic situations. Recent studies propose to use reinforcement learning (RL) to search for more efficient traffic signal plans. However, all existing RL-based studies design the key elements - reward and state - in a heuristic way. This results in highly sensitive performances and a long learning process.

To avoid heuristic design of RL for traffic signal control, we are the first to connect RL with recent studies in transportation research. Our method is inspired by the state-of-the-art method max pressure (MP) in the transportation field. The reward design of our method is well supported by the theory in MP, which can be proved to be maximizing the throughput of the traffic network, i.e., minimizing the overall network travel time. We also justify the concise state representation which can fully support the optimization of the proposed reward function. Through comprehensive experiments, we demonstrate that our method can outperform both convention



(a) Performance w.r.t. reward

(a) Convergence w.r.t. state

Figure 1: Performance of RL approaches is sensitive to reward and state. (a) A heuristic parameter tuning of reward function could result in different performances. (b) The method with a more complicated state (IntelliLight [32] w/ neighbor) has a longer learning time but does not necessarily converge to a better result.

CCS CONCEPTS

• **Computer systems organization** → **Embedded systems**; *Redundancy*; Robotics; • **Networks** → Network reliability.

KEYWORDS

Deep reinforcement learning, traffic signal control, multi-agent system

1 INTRODUCTION

Traffic signals coordinate the traffic movements at the intersection and a smart traffic signal control algorithm is the key for transportation efficiency. Traffic signal control has remained as an active research topic because of the high complexity of the problem. The traffic situations are highly dynamic and require the traffic signal plans to be able to adjust to different situations.

Permission to make digital or hard copies of all or part of this work for personal or classroom use is granted without fee provided that copies are not made or distributed for profit or commercial advantage and that copies bear this notice and the full citation on the first page. Copyrights for components of this work owned by others than ACM must be honored. Abstracting with credit is permitted. To copy otherwise, or republish, to post on servers or to redistribute to lists, requires prior specific permission and/or a fee. Request permissions from [permissions@acm.org](https://permissions.acm.org).

KDD '19, August 4–8, 2019, Anchorage, AK, USA

© 2019 Association for Computing Machinery.

ACM ISBN 978-1-4503-6201-6/19/08...\$15.00

<https://doi.org/10.1145/3292500.3330949>

Recently, people start to investigate reinforcement learning (RL) techniques for traffic signal control. Recent studies have shown the superior performance of RL technique over traditional transportation approaches [1, 2, 4, 26, 32, 33]. The biggest advantage of RL is that it directly learns how to take the next actions by observing the feedback from the environment after previous actions.

One most serious issue of current RL-based traffic signal control approaches is that the setting is often heuristic and lacks proper theoretical justification from transportation literature. This often results in highly sensitive performance w.r.t. the setting and leads to long learning process. We elaborate on this issue by examining two fundamental elements in RL setting: reward and state.

First, various reward designs have been proposed. The reason that the reward varies in literature is that travel time, the ultimate objective, is hard to optimize directly. Travel time is a long-term reward after a sequence of actions and the effect of one action can hardly be reflected in terms of travel time. People often choose short-term rewards like queue length or delay to approximate the travel time [31]. So the reward function is often defined as a weighted sum of these terms [6, 9, 10, 26, 32]. However, as shown in Figure 1(a), tuning the weights on these terms could lead to different results. None of the existing studies has discussed how to define the reward by connecting with the existing transportation method.

Second, existing RL methods have a trend of using more complicated state representation. Recent studies use visual images to describe the full traffic situation at the intersection [26, 32], which results in the dimension of the state in the scale of thousands. However, as shown in Figure 1(b), complicated state definitions increase the learning time and may not necessarily bring significant gain. Note that we are not claiming that additional information is always

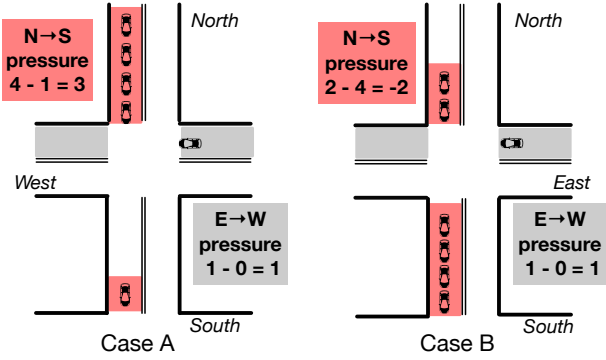


Figure 2: Illustration of max pressure control in two cases. In Case A, green signal is set in the North→South direction; in Case B, green signal is set in the East→West direction.

not helpful. The choice of the state depends on the reward setting. Based on the reward design of IntelliLight [32], neighboring information is not necessary in the case we shown in Figure 1(b). The question is, could we justify theoretically how much information is enough in state definition in order to optimize the reward function?

The challenges we face in RL motivate us to look for support in transportation approaches. In transportation literature, max pressure (MP) control is one of the state-of-the-arts in traffic signal control [17, 27]. The key idea of MP is to minimize the “pressure” of an intersection, which can be loosely defined as number of vehicles on entering lane minus the number of vehicles on exiting lane. Figure 2 illustrates the concept of pressure. By setting the objective as minimizing the pressure of intersections, MP is proved to maximize the throughput of the whole road network¹. However, the solution of MP is greedy which leads to locally optimal solutions.

Our proposed solution is based on RL technique but theoretically grounded by MP method. The connection between RL and MP is that both approaches can essentially be framed as an optimization problem. In RL, long term reward is the objective for optimization and the solution is derived from trial-and-error search. In MP, the objective is to minimize pressure and the solution is derived from a greedy algorithm. Intuitively, if we set our reward function the same as the objective of MP, we can achieve the same result as MP. We first prove that under the assumption of no physical queue expansion, both our method and MP are maximizing throughput of the network. We further show that our method can relax the assumption on queue expansion and the conclusion still holds.

To further address the challenge on state design, we describe the system dynamic using the state features based on MP. MP provides evolution equations to formulate the state transition of the traffic as a Markov chain [29]. In RL, the Markov decision process formally describes the dynamic of an environment. By including the variables from the evolution equation into state definition in RL, the state is a sufficient statistic for the system dynamic.

We conduct comprehensive experiments using both synthetic data and real data. We test our method in different scenarios of traffic flow and network structure. The evaluation is conducted through traffic simulator. We demonstrate the power of RL methods over

traditional transportation approaches because RL optimizes the objective through trial and error. Our method also consistently outperforms state-of-the-art RL methods, which shows that theoretically supported reward design is necessary and the concise design of state leads to efficient learning process.

2 RELATED WORK

Individual Traffic Signal Control. Individual traffic signal control has been investigated extensively in the field of transportation. These methods try to optimize the travel time or delay of vehicles [5, 11, 12, 16, 24], building on the assumption that vehicles are arriving and moving in a specific pattern. Recently, reinforcement learning based methods attempt to address this problem by directly learning from the data [19, 33]. Earlier work using tabular Q-learning [3, 9] can only deal with discrete state representations. Recent work using deep Q-learning [15, 26, 32] and policy gradient [7, 21] can cope with more complex continuous state representation, and hence have shown better performance.

Conventional Multi-intersection Traffic Signal Control. Conventional multi-intersection control usually requires the intersections to have the same cycle length, coordination can be achieved by setting a fixed offset (i.e., the time interval between the beginnings of green lights) among all intersections [25] in grid networks with homogeneous blocks. In fact, it is not an easy task to even provide coordination along an arterial, given traffic of opposite directions usually cannot be facilitated simultaneously. To solve this problem, some optimization-based methods [18, 22] are developed to minimize vehicle travel time and/or the number of stops at multiple intersections. Systems like SCATS and SCOOT also have internal selection or optimization processes to modify cycle length, phase splits and offsets [13]. Instead of optimizing offsets, max-pressure [27, 29] aims to maximize throughput of the network so as to minimizing the travel time. However, these approaches still rely on assumptions to simplify the traffic condition, and do not guarantee optimal results in the real world.

RL-based Multi-intersection Traffic Signal Control. Since recent advances in RL improve the performance on isolated traffic signal control [26, 32], efforts have been made to design strategies that control multiple intersections. *One way* is to consider explicit coordination mechanisms between learning agents using coordination graphs [14, 26], extending [33] using max-plus algorithm. Since all the above methods need to negotiate between the agents in the whole network, they are computationally expensive. *Another way* is to use individual RL agents to control the traffic signals in the multi-intersection system [4, 8, 10]. These methods are more scalable, since each agent makes its own decision based on the information from itself and neighboring intersections without explicit coordination. Our proposed method also follows this direction. However, none of the existing studies justified their reward and state design in a connection with traditional transportation methods.

In this sense, decentralized methods may be more scalable and practicable. Decentralized methods make use of isolated traffic signal control methods, using the information from both target and surrounding intersections. They are computationally less demanding because they only need and maintain relevant information from

¹Maximizing throughput equals to minimizing travel time under certain conditions and minimizing travel time is the final goal for most traffic signal control problems.

surrounding intersections. By plugging new intersection controllers into the system, the decentralized systems are easy to scale.

However, decentralized methods assume relatively static traffic environments, and are hence far from the real case. What's more, they only focus on rewards and overlook the adaptability of the algorithms to the real traffic. Therefore, they cannot interpret why the learned light signal changes corresponding to the traffic. In this paper, we try to test the algorithms in different traffic settings and add more interpretations other than reward. As far as we know, it is the first time that the policy learned by the reinforcement learning control agents are interpreted using the traditional transportation coordination method on an arterial.

3 PRELIMINARIES

Definition 3.1 (Entering lane and exiting lane of an intersection). An entering lane for an intersection is the lane where the traffic enters the intersection. An exiting lane for an intersection is the lane where the traffic leaves the intersection. We denote the set of entering lanes and exiting lanes of intersection as L_a and L_e respectively.

Definition 3.2 (Traffic movement). A traffic movement is defined as the traffic traveling across an intersection from one entering lane to an exiting lane. We denote a traffic movement from lane l to lane m as (l, m) .

Definition 3.3 (Phase). A phase is defined as a group of allowed traffic movements during a period of time. We denote a phase as $p = \{(l, m) | a(l, m) = 1\}$, where $l \in L_a$ and $m \in L_e$. $a(l, m) = 1$ indicates the green light is on for movement (l, m) , and $a(l, m) = 0$ indicates the red light is on for movement (l, m) .

In Figure 3, there are twelve entering lanes and twelve exiting lanes in the intersection. Four phases are used to control the traffic movements for the intersection: *WE-Straight* (Going Straight from West and East), *SN-Straight* (Going Straight from South and North), *WE-Left* (Turning Left from West and East), *SN-Left* (Turning Left from South and North). Specifically, *WE-Left* allows two traffic movements. When phase #2 is activated, the traffic from l_E and l_W is allowed to turn left to corresponding exiting lanes.

Definition 3.4 (Pressure of movement, pressure of intersection). The pressure of a movement is defined as the difference of vehicle density between the upstream lane and downstream lane. The vehicle density of a lane is defined as $x(l)/x_{max}(l)$, where $x(l)$ is the number of vehicles on lane l , $x_{max}(l)$ is maximum permissible vehicle number on l . We denote the pressure of movement (l, m) as

$$w(l, m) = \frac{x(l)}{x_{max}(l)} - \frac{x(m)}{x_{max}(m)} \quad (1)$$

If all the lanes have the same maximum capacity x_{max} , then $w(l, m)$ is simply indicating the difference between the upstream and downstream number of vehicles.

The pressure of an intersection i is defined as the sum of the absolute pressures over all traffic movements, denoted as:

$$P_i = \sum_{(l, m) \in i} |w(l, m)| \quad (2)$$

In Figure 2, the pressure of the intersection in Case A is $3 + 1 = 4$, where as the pressure of intersection in Case B is $2 + 1 = 3$. In general,

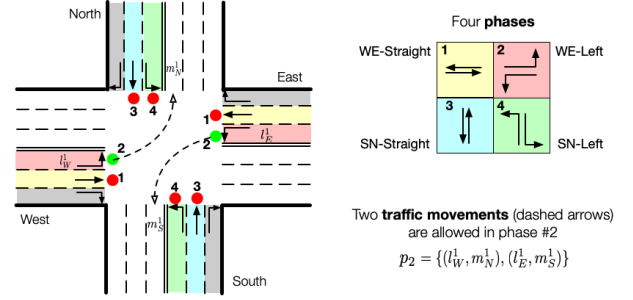


Figure 3: Phase and traffic movements in traffic signal control problem. Phase #2 is set in the example.

the pressure P_i indicates the degree of disequilibrium between the upstream and downstream vehicle density. The larger P_i is, the more unbalanced the distribution of vehicles is.

Problem 1 (Multi-intersection traffic signal control). In our problem, each intersection is controlled by an RL agent. At each time step t , agent i observes from the environment as its state o_i^t . Given the vehicle distribution and current traffic signal phase, the goal of the agent is to give the optimal action a (i.e., which phase to set), so that the reward r (i.e., the smoothness of the traffic) can be maximized.

4 METHOD

4.1 Agent Design

First, we introduce the state, action and reward design for an agent that controls an intersection.

- **State (Observation).** Our state is defined for one intersection, which equals to the definition of observation in multi-agent RL. It includes the current phase p , the number of vehicles on each exiting lane $x(m)$ ($m \in L_e$), and the number of vehicles on each segment of every entering lane $x(l)_k$ ($l \in L_a, k = 1 \dots K$). In this paper, each lane is evenly divided into 3 segments ($K = 3$), and we denote the segment nearest to the intersection as the first segment $x(l, \cdot)_1$.

- **Action.** At time t , each agent chooses a phase p as its action a_t from action set \mathbf{A} , indicating the traffic signal should be set to phase p . In this paper, each agent has four permissible actions: *WE-Straight* (Going Straight from West and East), *SN-Straight* (Going Straight from South and North), *WE-Left* (Turning Left from West and East), *SN-Left* (Turning Left from South and North). Each action candidate a_i is a one-hot vector representing a phase. Note that in the real world the signal phases may organize in a cyclic way, while our action makes the traffic signal plan more flexible. Also, there may be different number of phases in the real world, four phases is not a must; it can also include only two phases: *WE-Straight*, *SN-Straight*.

- **Reward.** As is shown in Equation (3), we define the reward r_i using the **pressure** P_i of the intersection i as

$$r_i = -P_i \quad (3)$$

where P_i is the pressure of intersection i , as defined in Equation (2).

Intuitively, the pressure P_i indicates the degree of disequilibrium between the upstream and downstream vehicle density. By minimizing P_i , the vehicles within the system can be evenly distributed.

Then the green light is effectively utilized so that the throughput is optimized.

4.2 Learning Process

In this paper, we adopt Deep Q-Network (DQN) as function approximator to estimate the Q-value function. To stabilize the training process, we maintain an experience replay memory as described in [20] by adding the new data samples in and removing the old samples occasionally. Periodically, the agent will take samples from the memory and use them to update the network.

5 JUSTIFICATION OF RL AGENT

To theoretically support the efficacy of our proposed method, we provide the proof of the design of the reward and state by showing that in a simplified transportation system, (1) the states we use can fully describe the system dynamics, and (2) using Equation (3) as reward function in RL is equivalent to optimizing travel time as in the transportation methods. Consider the arterial scenario described in Example 5.1.

Example 5.1. Figure 4 associates a distinct traffic movement with each entering lane $l \in L_a$ and each $m \in Out_l$, where Out_l is the set of lanes output from lane l . Follow the notations from [29], let $x(l, m)(t)$ be the associated number of vehicles at beginning of period t , $X(t) = \{x(l, m)(t)\}$ is the *state* of the movement network, which we regard as states o^t corresponding with Section 4.1. There are three variables that we consider independent of $X(t)$:

- Turning ratio $r(l, m)$: For each l and time t , $r(l, m)$ is iid random variables with mean value equal to probability $R(l, m)$.
- Discharging rate $c(l, m)$: For each (l, m) and time t , the queue discharging rates $c(l, m)$ are non-negative bounded iid random variables, i.e., $c(l, m) \leq C(l, m)$, $C(l, m)$ denotes the saturation flow rate.

At the end of each period t , an action $p^t = \{(l, m)|a^t(l, m), l \in L_a\}$ must be selected from the action set A^t as a function of X^t for use in period $(t + 1)$, indicating the agent will give green light for movements from l to m , see bottom of Figure 4.

Some important notations of the paper are shown in Table 1.

Table 1: Notations

Notation	Meaning
L_a	set of entering lanes for an intersection
L_e	set of exiting lanes for an intersection
(l, m)	a traffic movement that a green signal is on from lane l to m
$x(l, m)$	number of vehicles leaving l and entering m
$x(l, m)_k$	number of vehicles on k -th segment of l
$x_{max}(m)$	maximum permissible vehicle number on lane m
$r(l, m)$	turning ratio of traffic movements from l to m
$c(l, m)$	discharging rate of movement (l, m)
$a(l, m)$	1 if the green light is on for movement (l, m) , otherwise 0

5.1 Justification of State Design

5.1.1 Traffic movement process as a Markov chain. The evolution equations of $X(t)$ is developed in [27]. For each (l, m) and t , the

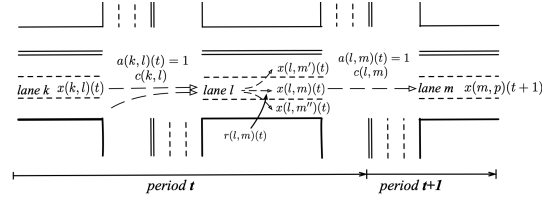


Figure 4: The transition of traffic movements

movement process consists of receiving and discharging. The evolution of $x(l, m)$ is captured by the following equation:

$$\begin{aligned}
 x(l, m)(t + 1) &= x(l, m)(t) + \underbrace{\sum_{k \in In_l} \min[c(k, l) \cdot a(k, l)(t), x(k, l)] \cdot r(l, m)}_{\text{receiving vehicles}} \\
 &\quad - \underbrace{\min\{c(l, m) \cdot a(l, m)(t), x(l, m)(t)\} \cdot 1(x(m) \leq x_{max}(m))}_{\text{discharging vehicles}}
 \end{aligned} \tag{4}$$

where In_l represent the set of lanes input to l . For the second term in Equation (4), when l is the receiving lane, up to $x(k, l)$ vehicles will move from k if $a(k, l)(t) = 1$ and they will join (l, m) if $r(l, m) = 1$. For the third term in Equation (4), when traffic movement (l, m) is actuated, i.e., $a(l, m)(t) = 1$, up to $x(l, m)$ vehicles will leave l and be routed to m if there is no blockage on lane m , i.e., $x(m) \leq x_{max}(m)$, where $x_{max}(m)$ means the maximum permissible vehicle number on l on lane m .

Suppose the initial state $X(1) = x(l, m)(1)$ is a bounded random variable. Since $A(t) = a(l, m)(t)$ is a function of the current state $X(t)$, and since $c(l, m)$ and $r(l, m)$ are all independent of $X(1), \dots, X(t)$, the process $X(t)$ is a **Markov chain**. The transition probabilities of the chain depends on the control policy.

5.1.2 Full description on system dynamics with proposed state definition. We can modify the traffic movement equation from lane-level to segment-level. Assuming the vehicles change lanes for routing by the time it enters the lane l , we have $x(l, m) = x(l)$. The movement process on segment nearest to the intersection as following Equation (5).

$$\begin{aligned}
 x(l)_1(t + 1) &= x(l)_1(t) + x(l)_2(t) \\
 &\quad - \min\{c(l, m) \cdot a(l, m)(t), x(l)_1(t)\} \cdot 1(x(m) \leq x_{max}(m))
 \end{aligned} \tag{5}$$

where $x(l)_1$ is the number of vehicles on the segment, $x(l)_2$ is the number of vehicles on the outer segment.

Through the lane and segment movement evolution equation demonstrated above, the evolution of an individual intersection could be derived, which is a combination of the equations of all the connected lanes involved. Hence, for a single intersection i , $c(l, m)$ the saturation flow rate is the constant physical feature of each lane, $x(l)_1$, $x(l)_2$ and $x(m)$ are provided to the local agent as in our state definition.

5.2 Justification of Reward Design

5.2.1 Stabilization on traffic movements with proposed reward. Inspired by [27], we first relax its assumptions about physical queue expansion in the arterial. Then the goal of our RL agents is proven to

stabilize the queue length and thus maximizes the system throughput and minimizes the travel time of vehicles.

Definition 5.2 (Movement process stability). The movement process $X(t) = \{x(l, m)(t)\}$ is stable in the mean (and u is a stabilizing control policy) if for some $M < \infty$, Equation (6) holds. Movement stability in the mean implies that the chain is positive recurrent and has a unique steady-state probability distribution for all times T . E denotes expectation.

$$\sum_{t=1}^T \sum_{(l, m)} E[x(l, m)(t)] < M, \quad \forall T. \quad (6)$$

Definition 5.3 (Max-pressure control policy [27]). At each period t , the agent selects the action with maximum pressure θ at every state X : $\tilde{A}^*(X) = \operatorname{argmax}_{\tilde{A} \in \mathbf{A}} \theta(\tilde{A}, X)$ where the pressure definition of each action $\tilde{A} \in \mathbf{A}$ is shown as $\theta(\tilde{A}, X) = \sum_{l, m: a(l, m)=1} c(l, m) \cdot \tilde{w}(l, m)(X)$, where $\tilde{w}(l, m)(X) = x(l) - x(m)$ is the pressure of each movement. In the following part, we denote notations of max-pressure policy with hat, i.e., \hat{A} to differentiate with RL policy.

THEOREM 5.4. Without considering the physical queue expansion², action \tilde{A}^* selected by max-pressure control policy and action A^* selected by our RL policy is stabilizing the system whenever the average demand is admissible³,

Proof. For max-pressure control policy, Theorem 1 in [27] shows that given a time period $t = 1, \dots, T$ there exist $m < \infty$ and $\epsilon > 0$ such that under \tilde{A}^* : $\epsilon \cdot \frac{1}{T} \sum_{t=1}^T E[X(t)] \leq m + \frac{1}{T} \cdot E[X(1)]^2$, where $X(1)$ denotes the state when $t = 1$. We include it here to stay self-contained.

For an optimal RL control policy π , the agent selects the action A with maximum total reward Q^* at every state X as in Equation (7).

$$A^*(X) = \operatorname{argmax}_{A \in \mathbf{A}} Q^*(A, X) \quad (7)$$

The difference between the pressure definition in RL reward and max-pressure is that our RL agent use the weighted pressure considering maximum permissible vehicle number x_{max} as Equation (1). The stability also holds by simply replacing $x(l)$ with $x(l)/x_{max}(l)$.

THEOREM 5.5. Considering the physical queue expansion in the arterial environment, action A^* selected by our RL policy is also stabilizing the movement.

Different from [27], we establish the proof of Theorem 5.5 by relaxing the constraints of ignoring physical queue expansion in the arterial environment. Under arterial environment, there is:

- The maximum permissible vehicle number x_{max} on side street lane m^{side} is assumed to be infinity, the second term in Equation (1) is zero, thus we have $w(l, m^{side}) = \frac{x(l)}{x_{max}(l)} > 0$.

- When the the downstream lane m^{main} along the arterial is saturated, the second term in Equation (1) is approximately 1 because of the queue expansion, thus phase weight $w(l, m^{main}) \approx \frac{x(l)}{x_{max}(l)} - 1 < 0$.

²“Without physical queue expansion” means the vehicles will be considered to have no physical length in a queue.

³Intuitively, an admissible demand means the traffic demand can be accommodated by traffic signal control strategies, not including situations like long-lasting over-saturated traffic that requires perimeter control to stop traffic from getting in the system.

This means when we consider the physical queue expansion in the arterial, $w(l, m^{side}) > w(l, m^{main})$, the control policy will prohibit letting more vehicles pushing into the downstream intersection thus prevent the queue spill back and blocks the movements of vehicles in other phases. Accordingly, M in Equation (6) is now set to be $M \leq x_{max}$.

5.2.2 Connection to throughput maximization and travel time minimization. Given that the traffic movement process of each intersection is stable, the system is accordingly stable. In an arterial environment without U-turn, vehicles that move from lane m to l would not move from l to m again, i.e., between $x(m, l)$ and $x(l, m)$ only one of them can exist under arterial network. Then the actions that RL agents take will not form grid lock or block the network, thus can efficiently utilize the green time. Within the given time period T , our RL agent can provides the maximum throughput, thus minimize the travel time of all vehicles within the system.

6 EXPERIMENT

We conduct experiments on CityFlow⁴, an open-source traffic simulator which supports large-scale traffic signal control. After the traffic data being fed into the simulator, a vehicle moves towards its destination according to the setting of the environment. The simulator provides the state to the signal control method and executes the traffic signal actions from the control method.⁵

6.1 Dataset Description

Both synthetic and real-world traffic flow data are used in our experiments. In a traffic dataset, each vehicle is described as (o, t, d) , where o is origin location, t is time, and d is destination location. Locations o and d are both locations on the road network. Traffic data is taken as input for simulator. All the data contains bi-directional and dynamic flows with turning traffic.

- Synthetic data. Four different configurations are tested, detailed in Table 2. This data is synthesized from statistical analysis of real-world traffic pattern in Jinan and Hangzhou.

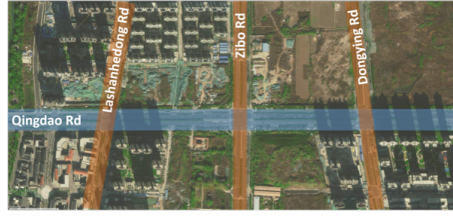
- Real-world data. We collect six representative traffic flow data from three cities to evaluate the performance of our proposed model, i.e., 1) Beaver Avenue in State College, USA, 2) Qingdao Road in Jinan, China, and 3) four avenues in Manhattan, New York City, USA. Figure 5 shows the aerial view on these arterials. Detailed statistics of these datasets are listed in Table 3.

Table 2: Configurations for synthetic traffic data

Config	Demand pattern	Arrival rate (vehicles/h/road)	Volume
1. Light-Flat	Flat	Arterial : 600	(Light)
2. Light-Peak	Peak	Side-street: 180	
3. Heavy-Flat	Flat	Arterial: 1400	(Heavy)
4. Heavy-Peak	Peak	Side-street : 420	

⁴<http://cityflow-project.github.io>

⁵Codes, public datasets and their preprocessing and statistical details can be found at the authors' website.



(a) Qingdao Road in Jinan, China:
a 3-intersection arterial with bidirectional traffic
on both the arterial and the side streets.



(b) Beaver Avenue in State College, Pennsylvania, USA:
a 5-intersection arterial with unidirectional traffic on the arterial
and bidirectional traffic on the side streets.



(c) 8-th, 9-th, 10-th and 11-th Avenue in New York City, USA:
four 16-intersection arterials with uni-directional traffic
on both the arterial and the side streets.

Figure 5: Real-world arterials for experiment.

Table 3: Data statistics of real-world traffic dataset

Dataset	Arrival rate (vehicles/h)				# of inter- sections
	Mean	Std	Max	Min	
Qingdao Rd.Jinan	3338.83	221.58	2748	3864	3
Beaver Ave., State College	2982.33	359.70	2724	3491	5
8-th Ave., NYC	6790.04	32.34	4968	7536	16
9-th Ave., NYC	4513.06	25.88	4416	6708	16
10-th Ave., NYC	6083.90	25.61	2892	5016	16
11-th Ave., NYC	4030.79	24.08	2472	4536	16

6.2 Experimental Settings

6.2.1 Environmental settings. Different road networks are configured. Besides a six-intersection arterial on which we mainly experiment, arterials with larger scale and heterogeneous intersections (in Figure 7) are also tested.

The free-flow speed on the road segments is set to 40 kilometers/hour. Vehicles can always turn right when there is no conflicting traffic. Every time the phase switches, a 5-second combined yellow and all-red time are followed to clear the intersection.

6.2.2 Evaluation metric. Following existing studies [32], we use the average **travel time** in seconds to evaluate the performance. Average travel time of all the vehicles is the most frequently used measure in transportation field [23], which is calculated as the average travel time of all vehicles spent in the system.

6.2.3 Compared methods. We compare our model with the following two categories of methods: transportation methods and RL methods. Note that all methods are carefully tuned and their best results are reported (except the offsets of FixedTime because of its random nature).

Conventional transportation baselines:

- **FixedTime:** Fixed-time with random offset [23]. Each phase has fixed time of 15 seconds. For uni-directional traffic, there are only 2 phases (WE-straight, SN-straight). For traffic with turning vehicles, there are 4 phases.

- **GreenWave** [23]: This policy is an optimal solution for uni-directional and uniform traffic on the arterial. It requires that all intersections share the same cycle length, which is the minimum value of the cycle length for individual intersections calculated using Webster’s theory [30] (see Section ??). The phase split percentage equals to the percentage between the demand of a designated phase and total demand. Offsets between intersections are equivalent to the free-flow travel time between two consecutive intersections. This is the most classical method in transportation field to implement coordination.

- **MaxPressure:** Max pressure control [28] is a state-of-the-art network-level traffic signal control method, which greedily chooses the phase with the maximum pressure (a pre-defined metric about upstream and downstream number of vehicles).

RL baselines:

- **IntelliLight** is an individual deep reinforcement learning approach proposed in [32]. This method does not consider neighbor information in state and uses a reward with mixed components.

- **GRL** is a coordinated reinforcement learning approach for multi-intersection control [26]. Specifically, the coordination is to design a coordination graph and to learn the joint local Q-function on two adjacent intersections directly.

6.3 Performance Comparison

Table 4 reports our experimental results using synthetic data under six-intersection arterial and real-world data *w.r.t.* average travel time. We have the following findings:

(1) Conventional transportation methods (FixedTime, GreenWave and MaxPressure) give poor performance. This is because the traffic in these settings is dynamic. Conventional methods, which

Table 4: Performance comparison between all the methods in the arterial with 6 intersections w.r.t. average travel time (the lower the better). Top-down: conventional transportation methods, learning methods, and our proposed method.

	Synthetic traffic				Real-world traffic					
	LightFlat	LightPeak	HeavyFlat	HeavyPeak	Qingdao Rd., Jinan	Beaver Ave., State College	8th Ave., NYC	9th Ave., NYC	10th Ave., NYC	11th Ave., NYC
FixedTime	93.29	109.50	325.48	246.25	317.40	336.29	432.60	469.54	347.05	368.84
GreenWave	98.39	124.09	263.36	286.85	370.30	332.06	451.98	502.30	317.02	314.08
MaxPressure	74.30	82.37	262.26	225.60	567.06	222.90	412.58	370.61	392.77	224.54
GRL	123.02	115.85	525.64	757.73	238.19	455.42	704.98	669.69	676.19	548.34
IntelliLight	65.07	66.77	233.17	258.33	58.18	338.52	471.30	726.04	309.95	340.40
PressLight	59.96	61.34	160.48	184.51	54.87	92.00	223.36	149.01	161.21	140.82

Table 5: Detailed comparison of our proposed state and reward design and their effects w.r.t. average travel time (lower the better) under synthetic traffic data.

	HeavyFlat	HeavyPeak
base	233.17	258.33
base+neigh	201.56	281.21
base+neigh+seg	200.28	196.34
PressLight	160.48	184.51

relies heavily on the predefined rules or prior knowledge about the traffic, may easily fail under the dynamic traffic scenarios.

(2) Our method PressLight outperforms all other RL methods. Though all the methods aim to learn to minimize the travel time, our reward design is proven to directly optimize towards it, while GRL and IntelliLight are using mixed reward which may distract the model from learning efficiently.

(3) When the traffic grows larger (Config 3,4 to 1,2), PressLight becomes much better than other baselines. Under heavy traffic, a poor control strategy would make downstream queue may easily spill back and the green time would be wasted. The reward design of our agents considers balancing the queues on all the intersections within the arterial, which makes the performance even superior as the traffic become larger.

6.4 Study of PressLight

Effects of variants of our proposed method. We consider several variations of our model as follows.

- **base.** Instead of using the distribution of the vehicles, base simply uses phase and number of vehicles on each entering lanes as its state (similar with IntelliLight), and uses the reward defined same as IntelliLight. This serves as a base model for later variants.
- **base+neigh.** Based on base, base+neigh adds the number of vehicles on exiting lanes to its state, which has more information about its downstream intersections than base agents.
- **base+neigh+seg.** Based on base+neigh, base+neigh+seg uses the phase, the number of segments' vehicles on both entering and exiting lanes into its state, which is the same as our proposed state definition.
- **PressLight.** Our proposed method which further changes base+neigh+seg's reward to pressure.

Table 5 shows the performance of variants of our method:

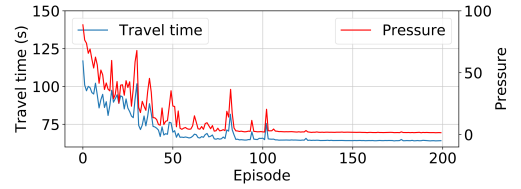


Figure 6: Convergence curve of average duration and our reward design (pressure). Pressure shows the same convergence trend with travel time.

(1) Giving more and more state information (base+neigh and base+neigh+seg) will boost the performance. This makes sense since (1) base+neigh is able to observe traffic condition on exiting lanes and helps to balance the queues for each intersection when there is congestion on downstream lanes; (2) base+neigh+seg has the information about vehicle distributions which is the key factor for agents to learn the best offset exactly.

(2) PressLight further outperforms base+neigh+seg if the reward changes to pressure. Instead of optimizing a reward that is not directly towards the travel time, our reward design is proved to be a surrogate of average travel time. This demonstrates the effectiveness of our proposed reward design.

Average travel time related to pressure. Figure 6 illustrates the convergence curve of our agents learning process w.r.t. the average reward and the average pressure of each round. We can see that the travel time is closely correlated with pressure.

6.5 Performance on mixed scenarios

6.5.1 Heterogeneous intersections. We employ our model to two heterogeneous arterials, as is shown in Figure 7. For intersections with 3 legs, we use zero-padding to complete the state. For intersections with different length of lanes, our method can handle this well since the state is independent of the lane length. Table 6 illustrates the performance of our model against MaxPressure.

6.5.2 Arterials with the different number of intersections and network. We employ our model to arterials with 6, 10 and 20 intersections under synthetic data. As is shown in Table 6, our model could achieve better performance over conventional transportation method MaxPressure and reinforcement learning method IntelliLight even when the number of intersections grows.

Table 6: Average travel time of different methods under arterials with different number of intersections and network.

	6-intersection arterial		10-intersection arterial		20-intersection arterial		Grid network	
	HeavyFlat	HeavyPeak	HeavyFlat	HeavyPeak	HeavyFlat	HeavyPeak	HeavyFlat	HeavyPeak
MaxPressure	262.26	225.60	129.63	129.63	310.95	271.39	539.67	485.03
IntelliLight	233.17	258.33	157.84	200.96	246.88	202.30	283.21	332.53
PressLight (ours)	160.48	184.51	88.88	79.61	155.84	188.92	251.02	262.46

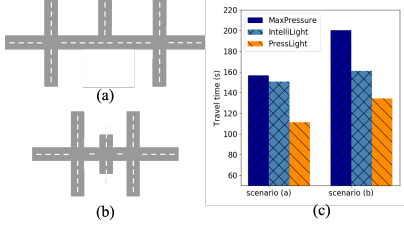


Figure 7: Average travel time of our method on heterogeneous intersections. (a) Different number of legs. (b) Different length of lanes. (c) Experiment results.

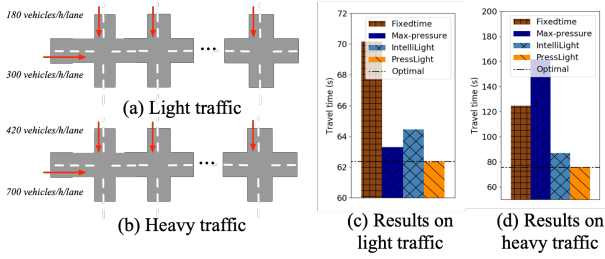


Figure 8: Performance comparison under uniform uni-directional traffic, where the optimal solution is known (GreenWave). Only PressLight can achieve the optimal.

We also test our model a network with 9 intersections (3×3 grid). Table 6 shows the experiment results and we can see that PressLight can outperform MaxPressure and IntelliLight under both traffic.

6.6 Case Study

Another desirable property of PressLight is its ability to automatically coordinate the offset between adjacent intersections. To demonstrate this, we show two examples. Under simplified uniform traffic, we show that our model has learned the optimal solution which could be justified by transportation theories. Under the real-world traffic, the learned offset is visualized to reveal this property.

6.6.1 Synthetic traffic on uniform, uni-directional traffic flow. In this section, we perform experiments on the arterials with six homogeneous intersections under two traffic settings. One is for light traffic (arterial demand: 300 vehicle/hour/lane, side-street demand: 180 vehicle/hour/lane) and one is for heavy traffic (arterial demand: 700 vehicle/hour/lane, side-street demand: 420 vehicle/hour/lane). Both of them are uniform, uni-directional traffic without turning traffic. Under these simplified scenarios, the optimal solution is known as GreenWave in transportation area as stated in [23]. As the optimal solution under these settings, GreenWave’s policy contains three parts: the offsets between intersections, the cycle length and the phase split, which requires several prior knowledge to calculate them. The offset Δ equals to the block length l between

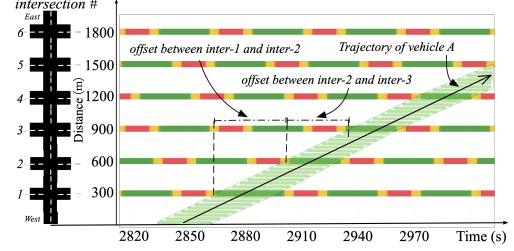


Figure 9: Offsets between intersections learnt by RL agents under uni-directional uniform traffic (700 vehicles/hour/lane on arterial)

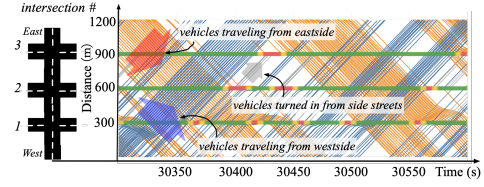


Figure 10: Space-time diagram with signal timing plan to illustrate the learned coordination strategy from real-world data on the arterial of Qingdao Road in the morning (around 8:30 a.m.) of August 6th.

two consecutive intersections divided by free-flow speed v , and the optimal phase split ratio is equal to the ratio of the demand for a designated phase and total demand. In our experiments, $l \approx 300$ m, $v \approx 10$ m/s, hence, the optimal offset should be $\Delta \approx 30$ s, and the optimal phase split should be 1:0.6 (WE-Straight:SN-Straight).

Performance comparison. We compared PressLight with all aforementioned baselines and report their results in Figure 8. We can find that given GreenWave is the optimal solution, only our method PressLight achieves the same performance as GreenWave in both settings. This demonstrates that our RL agents can learn the optimal policy under these simplified scenarios.

Policy learned by RL agents. We use time-space diagrams to show the trajectories of vehicles and phase plans of traffic signal controllers. In a time-space diagram like Figure 9, the x-axis is the time and the y-axis is the distance (from a reference point, here we use the westernmost point as the reference point). As it is shown in Figure 9, there are six bands with green-yellow-red colors indicating the changing phases of six intersections. The black line with arrow is the trajectory of a vehicle, where the x-axis tells the time and the y-axis tells the location. Vehicles that travel within the green dashed area will experience green wave. For example, vehicle A enters the system at 2850 second and travelled through 5 intersections at 3000 second, experiencing consecutive green lights during its trip. The slope indicates speed of the vehicle.

We have several observations:

(1) Our RL agents can learn the optimal phase split as Green-Wave. As is shown in Figure 9, our method learns optimal phase split (approximately 1:0.6, with 25 seconds of *WE-Straight*, 15 seconds of *SN-Straight*, and 10 seconds of yellow light).

(2) Our RL agents can learn the optimal offset and form a green wave. In Figure 9, the offset is approximately 30s between two consecutive traffic signals and a green wave can be seen (dashed green area in Figure 9). This demonstrates that our RL method can learn the optimal policy given from transportation methods.

6.6.2 Real-world traffic in Jinan. In this section, we make observations on the policies we learned from the real data for the arterial of Qingdao Road (*East* and *West* direction) during the morning peak hour (around 8:30 a.m.) on August 6th. In Figure 10, a time-space diagram is drawn with time on the horizontal axis and distance (from a reference point, here we use the westernmost point on the arterial as the reference point) on the vertical axis. Most of the blue and orange lines are straight, indicating most vehicles on the arterial are not stopped by red lights, which means our method can automatically form a green wave.

7 CONCLUSION

In this paper, we propose a novel RL method for multi-intersection traffic signal control on the arterials. We conduct extensive experiments using both synthetic and real data and demonstrate the superior performance of our method over the state-of-the-art. Especially, we draw a connection on the design between reinforcement learning with conventional transportation control methods. It is the first time the individual RL model automatically achieves coordination along arterial without any prior knowledge.

We acknowledge the limitations of our model and would like to point out several future directions. In our experiment, we did not model the behaviour of vehicles. The behaviour of vehicles (e.g., routing) in the real-world may change dynamically in response to traffic lights. Another direction can be reducing the cost of learning. Since RL is learning from trial-and-error, deploying an online updated RL model in real-world could be dangerous and costly.

ACKNOWLEDGMENTS

The work was supported in part by NSF awards #1652525, #1618448, and #1639150. The views and conclusions contained in this paper are those of the authors and should not be interpreted as representing any funding agencies.

REFERENCES

- [1] Monireh Abdoos, Nasser Mozayani, and Ana LC Bazzan. 2013. Holonic multi-agent system for traffic signals control. *Engineering Applications of Artificial Intelligence* 26, 5 (2013), 1575–1587.
- [2] Baher Abdulhai, Rob Pringle, and Grigoris J Karakoulas. 2003. Reinforcement learning for true adaptive traffic signal control. *Journal of Transportation Engineering* 129, 3 (2003), 278–285.
- [3] Baher Abdulhai, Rob Pringle, and Grigoris J Karakoulas. 2003. Reinforcement learning for true adaptive traffic signal control. *Journal of Transportation Engineering* 129, 3 (2003), 278–285.
- [4] Itamar Arel, Cong Liu, T Urbanik, and AG Kohls. 2010. Reinforcement learning-based multi-agent system for network traffic signal control. *IET Intelligent Transport Systems* 4, 2 (2010), 128–135.
- [5] Florence Boillot, Sophie Midenet, and Jean-Claude Pierrelee. 2006. The real-time urban traffic control system CRONOS: Algorithm and experiments. *Transportation Research Part C: Emerging Technologies* 14, 1 (2006), 18–38.
- [6] Tim Brys, Tong T Pham, and Matthew E Taylor. 2014. Distributed learning and multi-objectivity in traffic light control. *Connection Science* 26, 1 (2014), 65–83.
- [7] Noe Casas. 2017. Deep Deterministic Policy Gradient for Urban Traffic Light Control. *arXiv preprint arXiv:1703.09035* (2017).
- [8] ALCB Bruno Castro da Silva, Denise de Oliveria, and EW Basso. 2006. Adaptive traffic control with reinforcement learning. In *Conference on Autonomous Agents and Multiagent Systems (AAMAS)*. 80–86.
- [9] Samah El-Tantawy and Baher Abdulhai. 2010. An agent-based learning towards decentralized and coordinated traffic signal control. *IEEE Conference on Intelligent Transportation Systems, Proceedings, ITSC* (2010), 665–670. <https://doi.org/10.1109/ITSC.2010.5625066>
- [10] Samah El-Tantawy, Baher Abdulhai, and Hossam Abdelgawad. 2013. Multiagent reinforcement learning for integrated network of adaptive traffic signal controllers (MARLIN-ATSC): methodology and large-scale application on downtown Toronto. *IEEE Transactions on Intelligent Transportation Systems* 14, 3 (2013), 1140–1150.
- [11] Nathan H Gartner. 1983. *OPAC: A demand-responsive strategy for traffic signal control*. Number 906.
- [12] Jean-Jacques Henry, Jean Loup Farges, and J Tuffal. 1984. The PROLYN real time traffic algorithm. In *Control in Transportation Systems*. Elsevier, 305–310.
- [13] Cameron Kergaye, Aleksandar Stevanovic, and Peter T Martin. 2010. Comparative evaluation of adaptive traffic control system assessments through field and microsimulation. *Journal of Intelligent Transportation Systems* 14, 2 (2010), 109–124.
- [14] Lior Kuyner, Shimon Whiteson, Bram Bakker, and Nikos Vlassis. 2008. Multiagent reinforcement learning for urban traffic control using coordination graphs. *Machine learning and knowledge discovery in databases* (2008), 656–671.
- [15] Li Li, Yisheng Lv, and Fei-Yue Wang. 2016. Traffic signal timing via deep reinforcement learning. *IEEE/CAA Journal of Automatica Sinica* 3, 3 (2016), 247–254.
- [16] Xiaoyuan Liang, Xunsheng Du, Guiling Wang, and Zhu Han. 2018. Deep reinforcement learning for traffic light control in vehicular networks. *arXiv preprint arXiv:1803.11115* (2018).
- [17] Jennie Lioris, Alex Kurzshanskiy, and Pravin Varaiya. 2013. Adaptive Max Pressure Control of Network of Signalized Intersections. *Transportation Research Part C* 36, 22 (2013), 177–195.
- [18] John DC Little, Mark D Kelson, and Nathan H Gartner. 1981. MAXBAND: A versatile program for setting signals on arteries and triangular networks. (1981).
- [19] Patrick Mannion, Jim Duggan, and Enda Howley. 2016. An experimental review of reinforcement learning algorithms for adaptive traffic signal control. In *Autonomic Road Transport Support Systems*. Springer, 47–66.
- [20] Volodymyr Mnih, Koray Kavukcuoglu, David Silver, Andrei A Rusu, Joel Veness, Marc G Bellemare, Alex Graves, Martin Riedmiller, Andreas K Fidjeland, Georg Ostrovski, et al. 2015. Human-level control through deep reinforcement learning. *Nature* 518, 7540 (2015), 529.
- [21] Seyed Sajad Mousavi, Michael Schukat, Peter Corcoran, and Enda Howley. 2017. Traffic Light Control Using Deep Policy-Gradient and Value-Function Based Reinforcement Learning. *arXiv preprint arXiv:1704.08883* (2017).
- [22] Dennis I Robertson. 1969. TRANSYT: a traffic network study tool. (1969).
- [23] Roger P Roess, Elena S Prassas, and William R Mcshane. 2011. *Traffic Engineering*. Pearson/Prentice Hall.
- [24] Suvrajeet Sen and K Larry Head. 1997. Controlled optimization of phases at an intersection. *Transportation science* 31, 1 (1997), 5–17.
- [25] Thomas Urbanik, Alison Tanaka, Bailey Lozner, Eric Lindstrom, Kevin Lee, Shaun Quayle, Scott Beaird, Shing Tsoi, Paul Ryus, Doug Gettman, et al. 2015. *Signal timing manual*. Transportation Research Board.
- [26] van der Pol et al. 2016. Coordinated Deep Reinforcement Learners for Traffic Light Control. NIPS.
- [27] Pravin Varaiya. 2013. Max pressure control of a network of signalized intersections. *Transportation Research Part C: Emerging Technologies* 36 (2013), 177–195.
- [28] Pravin Varaiya. 2013. Max pressure control of a network of signalized intersections. *Transportation Research Part C: Emerging Technologies* 36 (2013), 177–195.
- [29] Pravin Varaiya. 2013. *The Max-Pressure Controller for Arbitrary Networks of Signalized Intersections*. Vol. 2. <https://doi.org/10.1007/978-1-4614-6243-9>
- [30] F. V Webster. 1958. Traffic signal settings. *Road Research Technical Paper* 39 (1958).
- [31] Hua Wei, Guanjie Zheng, Vikash Gayah, and Zhenhui Li. 2019. A Survey on Traffic Signal Control Methods. *CoRR abs/1904.08117* (2019). [arXiv:1904.08117](https://arxiv.org/abs/1904.08117)
- [32] Hua Wei, Guanjie Zheng, Huaxiu Yao, and Zhenhui Li. 2018. IntelliLight: A Reinforcement Learning Approach for Intelligent Traffic Light Control. In *Proceedings of the 24th ACM SIGKDD International Conference on Knowledge Discovery & Data Mining*. ACM, 2496–2505.
- [33] MA Wiering. 2000. Multi-agent reinforcement learning for traffic light control. In *Machine Learning: Proceedings of the Seventeenth International Conference (ICML'2000)*. 1151–1158.